*Journal of Applied Electrochemistry* **33**: 685–692, 2003.



# Kinetics of copper electrodeposition in the presence of triethyl-benzyl ammonium chloride

S. VARVARA[1], L. MURESAN[1,*], I.C. POPESCU[1] and G. MAURIN[2]
[1]*'Babes-Bolyai' University, Department of Physical Chemistry, Str. Arany Janos, no. 11, 3400 Cluj-Napoca, Romania*
[2]*Université 'Pierre et Marie Curie', Laboratoire de Physique des Liquides et Electrochimie, 4 Place Jussieu, 75252 Paris, France*
*(*author for correspondence, e-mail: limur@chem.ubbcluj.ro)*

Received 21 October 2002; accepted in revised form 10 April 2003

*Key words:* additives, copper electrodeposition, electrochemical impedance, triethyl-benzyl-ammonium chloride

**Abstract**

Quasi-steady state hydrodynamic voltammetry at a rotating-disc electrode and electrochemical impedance spectroscopy were used to investigate the influence of triethyl-benzyl-ammonium (TEBA) chloride on the kinetics of copper electrodeposition from sulphate acidic electrolytes. SEM and X-ray diffraction analysis were used to examine the morphology and the structure of copper deposits. The kinetic parameters ($i_0$, $\alpha_c$, $k_0$), obtained by both Tafel and Koutecky–Levich interpretations lead to the conclusion that TEBA acts as an inhibitor of copper electrodeposition process, as a consequence of its adsorption on the electrode surface. The influence of TEBA on the kinetics of copper electrodeposition was explained in terms of a reaction model confirmed by the simulated impedance spectra. TEBA acts only as a blocking agent competing for adsorption active sites of the cathodic surface with cuprous ions without changing the reaction pathway corresponding to the absence of the additive.

## 1. Introduction

Organic additives, such as thiourea [1–14], gelatine [4, 5] and animal glue [12] are widely used in copper electrodeposition since they can produce smooth and bright copper deposits. However, in certain conditions, thiourea, the most commonly used addition agent, may decompose at the cathodic surface and lead to contamination of the deposits with sulfur. For this reason the development of suitable brightening and levelling agents as substitutes for thiourea remains an interesting research direction.

Recently, a new additive IT-85, representing a mixture of ethoxyacetic alcohol and triethyl-benzyl-ammonium chloride (TEBA) was proved to be an efficient levelling agent in copper electrodeposition process [13]. To improve an understanding of the mechanism of action of IT-85 on the cathodic process, it was interesting to investigate, separately, the effect of TEBA on copper electrodeposition from sulfate electrolytes. On the other hand, in spite of the fact that the quaternary ammonium salts are known to act as blocking agents in metal electrocrystallization [15–17], there is little information, concerning the kinetic parameters of the cathodic process in their presence.

The aim of this study is to examine the effect of TEBA on the kinetics of copper electrodeposition from acidic sulfate electrolytes using electrochemical methods such as hydrodynamic voltammetry at a rotating disc electrode (RDE) and electrochemical impedance spectroscopy. Electrochemical results were correlated with those obtained from the examination of the cathodic deposits obtained by potentiostatic electrolysis. The morphology and the structure of the copper deposits were investigated using scanning electron microscopy (SEM) and X-ray diffraction analysis.

## 2. Experimental details

### 2.1. *Reagents*

A stock solution of acidic copper sulfate containing 30 g $l^{-1}$ $Cu^{2+}$ as $CuSO_4$ and 100 g $l^{-1}$ $H_2SO_4$ was prepared using pure reagents and distilled water. Solutions with various amounts of triethyl-benzyl-ammonium (TEBA) chloride concentration (0.5; 1 and 2 g $l^{-1}$) were prepared using the stock solution.

All reagents were Merck (Darmstadt, Germany) products of analytical grade of purity.

### 2.2. *Electrochemical measurements*

The experimental set-up consisted of a conventional three-electrode cell connected to a potentiostat (PS 3

Meinsberg, Germany) equipped with a data acquisition system (National Instruments AT MIO16 T5 acquisition board coupled to an IBM PC).

The amperometric measurements at the RDE with linear variation of rotation speed were performed at different electrode potentials, by scanning the electrode rotation speed between 100 and 2500 rpm with 20 rpm increments. The range of electrode potentials was chosen in the activation–diffusion control region of the quasi-steady state hydrodynamic voltammograms.

The working electrode was a copper disc electrode (dia. 3 mm). To ensure reproducibility between experiments, the exposed surface was polished with 600 and 1200 grit paper, and rinsed with distilled water. The counter electrode was a platinum foil and a saturated calomel electrode (SCE) was used as reference electrode.

All electrochemical measurements for copper electrodeposition were performed under potentiostatic conditions without ohmic drop compensation. The ohmic drop correction of the applied electrode potential was done by calculus using the electrolyte resistance determined from the electrochemical impedance spectra.

The impedance spectroscopy measurements were carried out in the 3.2 mHz–10 kHz frequency range, at different dc potentials chosen within the range −100 to −175 mV vs SCE. To attain the steady state, the electrode was rotated at 1000 rpm. To improve the accuracy, measurements were automatically repeated up to 20 times, especially for the high frequencies domain.

### 2.3. *Preparative electrolysis*

Small-scale potentiostatic electrolysis was performed in the absence and in the presence of different amounts of TEBA, at room temperature, employing a glass cell equipped with one vertical planar brass cathode and a platinum anode. In all cases, the potential was held constant at −0.175 V vs SCE during the deposition time of 45 min.

## 3. Results and discussion

### 3.1. *Effect of additives on the deposit morphology*

As can be seen from Figure 1, the presence of TEBA changed significantly the morphology and structure of the copper deposit as compared with that obtained from the same solution in the absence of additive.

The X-ray diffraction analysis showed a change of the Cu deposits texture from (111), obtained in the absence of TEBA, to (110) found in its presence. The (110) texture proves an inhibition action exerted by the additive on the crystal growth process [13]. Consequently, the presence of TEBA induced a relative enhancement of the nucleation process, resulting in a finer grained deposit.

### 3.2. *Quasi-steady state hydrodynamic voltammetry at RDE*

The inhibition of the cathodic process induced by TEBA was confirmed by the hydrodynamic voltammetric measurements at copper RDE (Figure 2). The cathode polarization increases due to the TEBA adsorption at the electrode interface, a fact reflected by the progressive decrease of the cathodic current for a given electrode potential value.

At the same time, in the presence of TEBA, the nucleation was enhanced, as was observed from the increase in length of the initial part of the hydrodynamic voltammograms. The nucleation enhancement results in finer grained copper deposits, (Figure 1).

To obtain quantitative information about the kinetics of the copper electrodeposition in the presence of TEBA, the hydrodynamic voltammograms at the RDE were examined by using Tafel and Koutecky–Levich interpretations. For this purpose, the generally accepted kinetic scheme for copper electrodeposition from acid sulfate solutions [18]:

$$Cu^{2+} + e^- \rightarrow Cu^+ \qquad (R1)$$

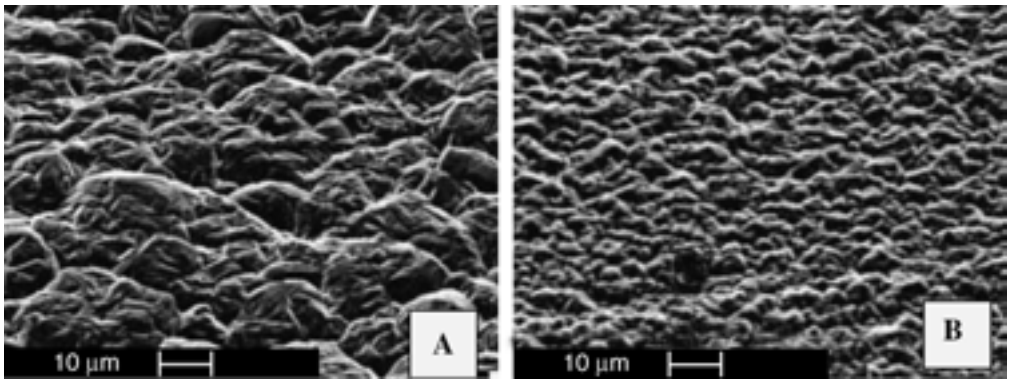


*Fig. 1.* SEM micrographs of copper deposits obtained at $E = -0.175$ V vs SCE in the absence (**A**) and in the presence (**B**) of 1 g $l^{-1}$ TEBA. Experimental conditions: electrolyte, 30 g $l^{-1}$ $Cu^{2+}$ and 100 g $l^{-1}$ $H_2SO_4$; rotation speed 1000 rpm.

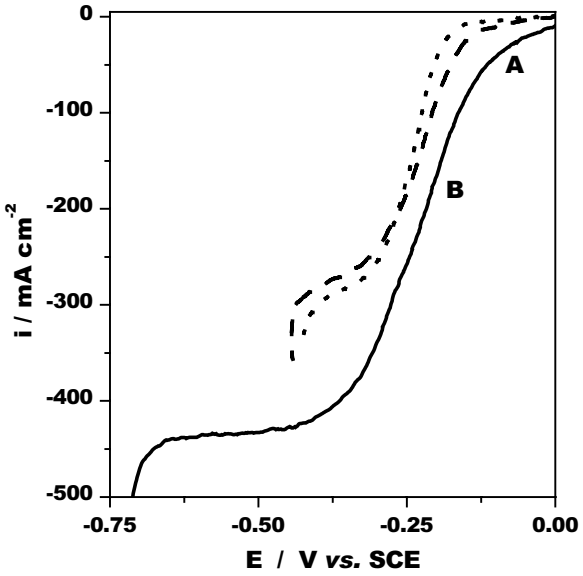


*Fig. 2.* Influence of TEBA concentration on the hydrodynamic voltammograms at RDE: (—) no additive; (-·-·-) 1 g $l^{-1}$TEBA; (···) 2 g $l^{-1}$ TEBA. Curves corrected for ohmic drop. Experimental conditions: scan rate 20 mV $s^{-1}$; rotation speed 1000 rpm; other conditions as in Figure 1.

*Table 1.* Kinetic parameters of the copper electrodeposition reaction in solutions without and with TEBA, determined by Tafel method

| TEBA concentration /g $l^{-1}$ | Transfer coefficient* $\alpha_c$ | Exchange current density* /mA $cm^{-2}$ | Corr. coeff. /No. of exp. points |
|---|---|---|---|
| 0 | 0.49 ± 0.01 | 6.0 ± 0.22 | 0.995/30 |
| 0.5 | 0.50 ± 0.02 | 1.2 ± 0.02 | 0.995/25 |
| 1 | 0.49 ± 0.01 | 1.1 ± 0.08 | 0.993/25 |
| 2 | 0.49 ± 0.01 | 0.4 ± 0.02 | 0.995/25 |

* With standard deviation.

$$Cu^{+} + e^{-} \rightarrow Cu \qquad (R2)$$

was adopted. Equation R1 is the rate controlling step.

The Tafel plots were constructed using the experimental data from the activation domain of the hydrodynamic voltammograms (region A, Figure 2). The calculated electrochemical kinetic parameters $\alpha_c$ and $i_0$ are presented in Table 1.

Another estimation of kinetic parameters $\alpha_c$ and $k_0$ corresponding to the heterogeneous electron transfer was attempted using amperometric measurements at RDE with linear sweep of the rotation speed. The constant electrode potential values were chosen from the activation-diffusion region (region B, Figure 2). The $I^{-1}$ vs $\omega^{-1/2}$ dependence, depicted in Figure 3, was used to calculate the electrochemical heterogeneous rate constant. A Tafel type representation (Figure 3 inserts) allowed the estimation of $\alpha_c$ and $k_0$ kinetic parameters (Table 2).

A comparison of the results presented in Tables 1 and 2, reveals that both Tafel and Koutecky–Levich methods lead to $\alpha_c$ values close to 0.5, irrespective of the TEBA presence or absence. The relative invariance of $\alpha_c$, observed for increasing TEBA concentrations, suggests

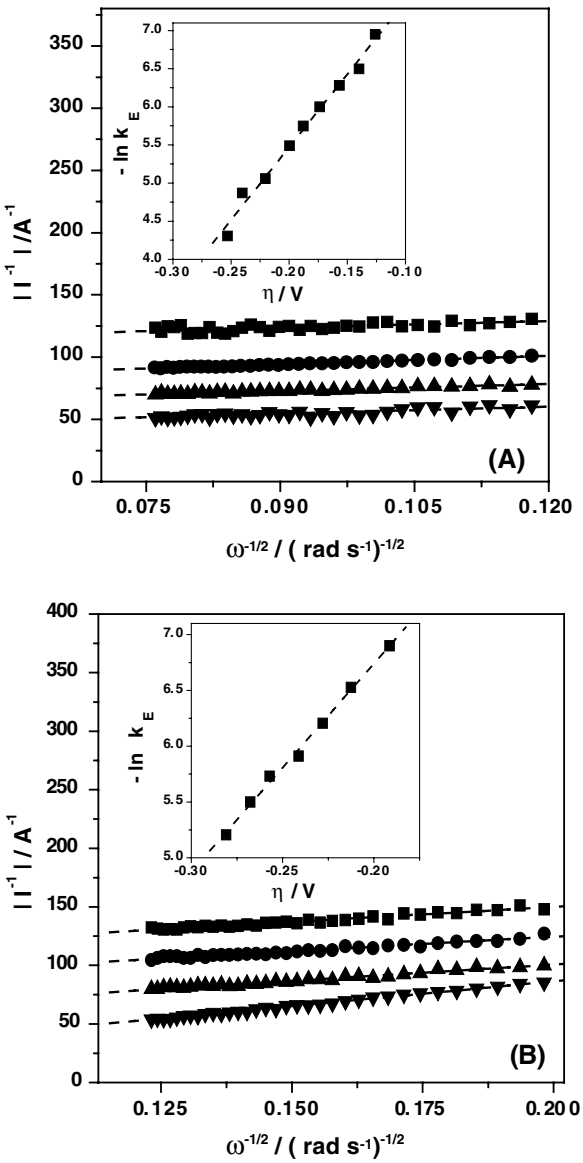


*Fig. 3.* $1/I$ against $\omega^{-1/2}$ dependence in the absence (**A**) and in the presence of 1 g $l^{-1}$ TEBA (**B**), at constant potentials chosen from the mixed-control region: (**A**) (■) −225, (●) −250, (▲) −300 and (▼) −375 mV vs SCE. (**B**) (■) −250, (●) −275, (▲) −325 and (▼) −400 mV vs SCE. **Inserts**: Variation of electrochemical rate constant ($k_E$) with the overpotential ($\eta$).

that the Cu electrodeposition reaction pathway is not affected by the TEBA presence. On the other hand, the continuous decrease of $i_0$ values, induced by increasing TEBA concentrations, should be related to the inhibiting effect of the additive due to its adsorption on the copper electrode surface.

In the absence of additives but for similar electrolyte composition, $i_0$ values, obtained generally by the Tafel method, vary significantly from 3 to 10.5 mA $cm^{-2}$ [7–13, 19–21]. It was shown that these variations arise mainly from small inherent differences between the experimental conditions (surface state, solution contamination etc.), strongly affecting the kinetic parameter reproducibility [19]. In this context, the discrepancies between the $i_0$ values, obtained by Koutecky–Levich and

*Table 2.* Kinetic parameters of the copper electrodeposition reaction in solutions without and with TEBA, determined by Koutecky–Levich method

| TEBA concentration /g $l^{-1}$ | Transfer coefficient* $\alpha_c$ | Standard rate constant* $k_0 \times 10^5$/cm $s^{-1}$ | Exchange current density*,† $i_0$/mA $cm^{-2}$ | Corr. coeff. /No. of exp. points |
|---|---|---|---|---|
| 0 | 0.49 ± 0.02 | 10.9 ± 0.1 | 4.9 ± 0.2 | 0.993 / 9 |
| 0.5 | 0.50 ± 0.07 | 5.4 ± 0.1 | 2.4 ± 0.1 | 0.999 / 7 |
| 1 | 0.50 ± 0.01 | 3.0 ± 0.1 | 1.3 ± 0.1 | 0.998 / 7 |
| 2 | 0.52 ± 0.03 | 1.1 ± 0.4 | 0.5 ± 0.1 | 0.985 / 6 |

* With standard deviation.
† Calculated from $k_0$.

Tafel interpretations, are not large. Moreover, the continuous increase in the active surface area during copper electrodeposition, especially at high overpotentials used for Koutecky–Levich method, could be another reason for these discrepancies.

### 3.3. *Impedance measurements*

Complex-plane impedance diagrams, recorded in the absence and presence of different TEBA concentrations, exhibited two capacitive loops and a low-frequency inductive loop (Figure 4). No significant modification of the shape, type and number of the loops were observed for different values of d.c. potential and TEBA concentration, but variations of the apex frequency and of the loops diameter are evident.

To evaluate the values of the charge transfer resistance ($R_{ct}$) and double layer capacity ($C_d$) from the high frequency capacitive loop, the response of a Randles equivalent electric circuit was fitted to the experimental impedance data using a Levenberg–Marquardt nonlinear regression [22].

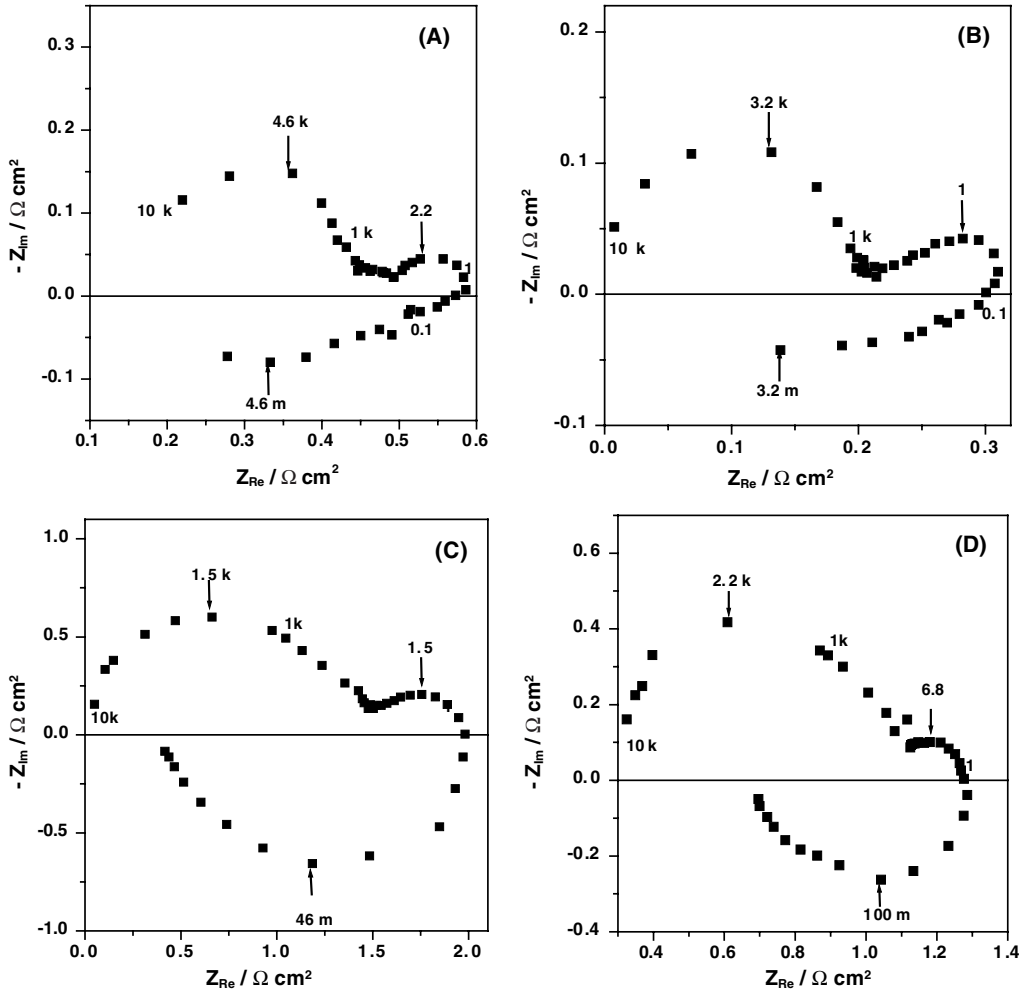


*Fig. 4.* Nyquist impedance diagrams for copper electrodeposition at different values of dc potential in the absence (**A**), (**B**) and in the presence of 1 g $l^{-1}$ TEBA (**C**), (**D**). Experimental conditions: electrode potential, −150 mV vs SCE (**A, C**); −175 mV vs SCE (**B, D**); rotation speed 1000 rpm. Frequencies are expressed in Hz.

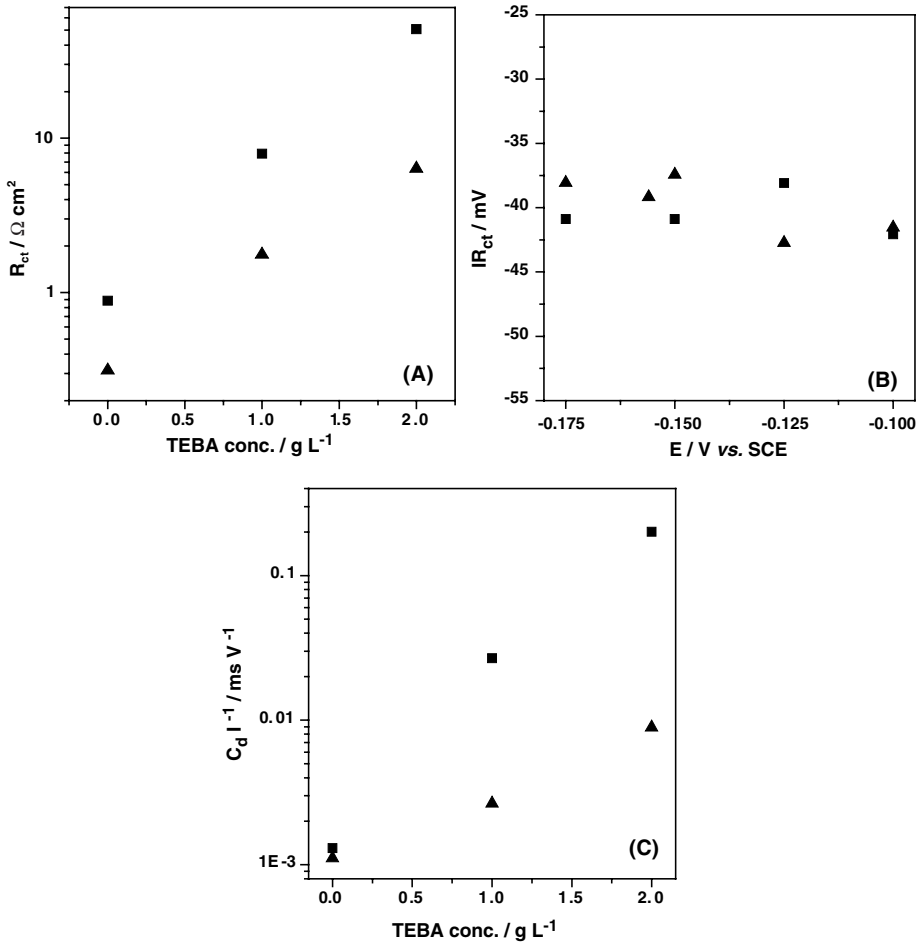


*Fig. 5.* Influence of TEBA concentration and of the electrode potential on the charge transfer resistance (**A**) and on the extensive parameters $IR_{ct}$ (**B**) and $C_d/I$ (**C**). Experimental conditions: electrode potential, (■) −100, and (▲) −175 mV vs SCE (**A, C**); (■) 0 g l$^{-1}$TEBA, (▲) 1 g l$^{-1}$ TEBA (**B**); rotation speed, 1000 rpm.

The charge transfer resistance increases significantly with TEBA concentration (Figure 5A), again confirming the inhibiting effect of the additive on the charge transfer step from the copper electrodeposition process.

In the presence of TEBA, a slight variation of the extensive parameter $IR_{ct}$ was observed for different dc potential values (Figure 5B). A comparison of this behaviour with that observed in the absence of TEBA proves that, within the investigated potential range, the presence of the additive has no effect on the charge transfer mechanism. This is in accordance with the invariance of the $\alpha_c$ values (Tables 1 and 2) observed in the presence of the additive. Consequently, it may be assumed that TEBA acts in the copper electrodeposition process only as a surface-blocking agent.

On the other hand, the calculated values of the extensive parameter $C_d/I$, reported for two values of the electrode potential, increase with TEBA concentrations (Figure 5C). This effect is the result of triethyl-benzyl-ammonium cation adsorption, resulting in an interfacial capacitance increase, and/or a current intensity decrease.

In the presence of TEBA, the apex frequency values of the intermediate-frequency capacitive loop increase with electrode polarization, showing that the corresponding process is potential activated (Figure 4). On this basis, and taking into account the results of Chassaing and Wiart for copper electrocrystallization on polycrystalline copper electrodes [23], the intermediate-frequency capacitive loop was attributed to a relaxation process of a charged adsorbed intermediate ($Cu^+_{ads}$).

The low-frequency inductive loop could be interpreted in terms of the electrode area relaxation due to the birth and growth of monolayers formed on the facets of the crystallites. The inductive loop originates from the lengthening of the distance corresponding to the propagation of edges, induced by the slow desorption of inhibiting adsorbate species [23, 24].

At a given dc potential (i.e., −175 mV vs SCE) the decrease of the time constant value of the inductive loop, observed in the presence of TEBA (Figure 4B and 4D), suggests an increase in the nuclei renewal rate, associated to an increase in the number of nuclei on the electrode surface. This conclusion is in accordance with the morphology of the copper deposits, showing a decrease in grain size in the presence of TEBA as compared with its absence (Figure 1). Thus, TEBA promotes the nucleation and inhibits the crystal growth process.

### 3.5. *Simulation of the electrode kinetics*

As already mentioned the copper electrodeposition process from acidic sulfate electrolytes occurs in two steps (R1) and (R2), both considered as irreversible reactions.

To simplify the mathematical model, the assumptions proposed by Wiart et al. [25, 26] for zinc electrodeposition were adopted for copper electrodeposition in the absence of additives:

(i) For the considered electrochemical reactions, the rates constant vary with the cathodic potential ($E$) according to the Tafel equation. Each reaction $i$ has a normalized rate constant $A_i = a_i \exp(-b_i(E_i - E_0))$, where $b_i = \alpha_i F/RT$ is the activation coefficient; $a_i$ includes both the rate constant, $k_i$, and the concentration of the reacting species, $c_i$ ($a_i = k_i c$); $E_0$ is an arbitrary chosen origin of potential ($E_0 = -0.1$ V vs SCE).

(ii) The adsorption process for the intermediate $Cu^+_{(ads)}$ follows the Langmuir isotherm.

(iii) The elementary steps of copper electrocrystallization will be disregarded. Consequently, this model will not explain the low-frequency loop ascribed to the nucleation-growth process.

(iv) For simplicity, the disproportionation reaction of cupric ions will be not considered.

Under these assumptions, the material and charge balances have been calculated as functions of the electrode coverage ($\theta$) by the adsorbed species $Cu^+_{(ads)}$:

$$\beta \frac{d\theta}{dt} = A_1(1-\theta) - A_2\theta \quad (1)$$

and

$$i = F[A_1(1-\theta) + A_2\theta] \quad (2)$$

where $\beta$ is the maximal surface concentration of copper atoms on the electrode surface ($\beta = 5.85 \times 10^{-8}$ mol cm$^{-2}$) [27, 28].

The faradaic impedance, defined as $1/Z_F = \Delta i/\Delta E$, was calculated using Equation 2 and the following relation:

$$-\frac{1}{Z_F} = \left.\frac{\partial i}{\partial E}\right|_\theta + \left.\frac{\partial i}{\partial \theta}\right|_E \frac{\Delta\theta}{\Delta E} \quad (3)$$

where the first term corresponds to the inverse of the charge transfer resistance $R_{ct}$ and the second one is due to the relaxation process of the electrode coverage.

The total electrode impedance was calculated considering $Z_F$ in parallel with the double-layer capacitance $C_d$, estimated from the apex of the high-frequency capacitive loop.

In the presence of TEBA, it was assumed that the reaction mechanism is essentially the same as in its absence, and the additive acts only as a blocking agent competing with cuprous ions for adsorption active sites of the cathodic surface. As a consequence, the electrode coverage should include two terms: one corresponding to the adsorbed $Cu^+$ ions and the other one to TEBA.

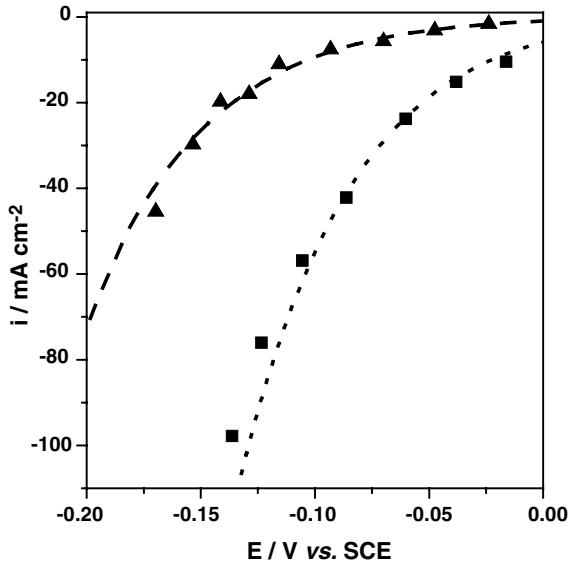


*Fig. 6.* Hydrodynamic voltammograms simulated with the sets of parameters from Table 3, in the absence (···) and in the presence of 1 g L$^{-1}$ TEBA (– – –). Symbols correspond to experimental points for absence (■) and presence of 1 g l$^{-1}$ TEBA (▲).

As can be seen from Figure 6, there is a good agreement between the simulated and the experimental steady-state hydrodynamic voltammograms, in the absence and presence of TEBA. The parameters used for the simulation are presented in Table 3.

The Nyquist experimental diagrams recorded for copper electrodeposition in the absence and in the presence of TEBA (Figure 4) have been compared with the calculated ones obtained using a Fortran program based on the above-described mathematical model (Figure 7) and the parameters specified in Table 3.

A semi-quantitative agreement between simulated and experimental data has been obtained for the current, the charge transfer resistance, the shape of Nyquist diagrams and the characteristic frequencies for the relaxation processes.

As expected, the best fitting was obtained, both in the absence and presence of TEBA, when the first step of the copper electrodeposition process was considered the rate-determining step ($a_1 < a_2$). The $k_1$ values used for simulation (Table 3) were found to be in agreement with

*Table 3.* Parameters used for the simulation of Nyquist impedance diagrams in the absence and in the presence of 1 g l$^{-1}$ TEBA

| Parameters* | Without additive | TEBA |
|---|---|---|
| $a_1$ | $5.1 \times 10^{-8}$ ($k_1 = 1.1 \times 10^{-4}$) | $8.9 \times 10^{-9}$ ($k_1 = 1.9 \times 10^{-5}$) |
| $b_1$ | 19 | 19 |
| $a_2$ | $7.8 \times 10^{-8}$ | $1.2 \times 10^{-8}$ |
| $b_2$ | 31 | 31 |
| $C_d$ | $56 \times 10^{-6}$ | $93 \times 10^{-6}$ |

* $a_i$/mol cm$^{-2}$ s$^{-1}$; $k_i$/cm s$^{-1}$; $b_i$/V$^{-1}$; $C_d$/F cm$^{-2}$.

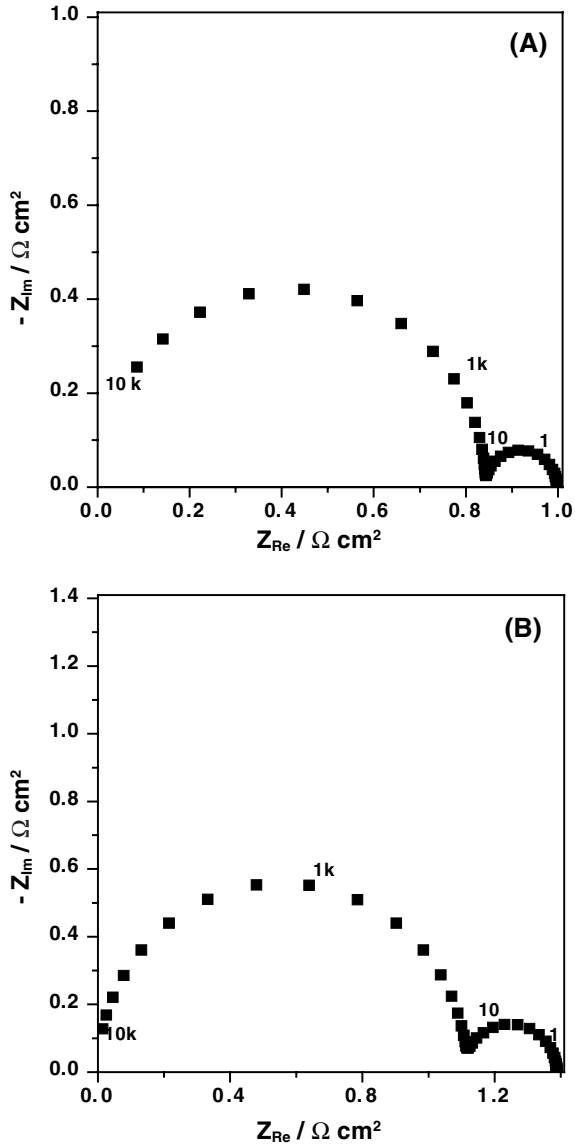


*Fig. 7.* Nyquist impedance plots, simulated in the absence of TEBA (**A**) Frequencies are expressed in #7 and in the presence of 1 g $l^{-1}$ TEBA, (**B**). Experimental conditions: electrode potential, −100 (**A**) and −175 mV vs SCE (**B**).

those determined using the Koutecky–Levich method. At the same time, the $k_1$ values used for simulation in the presence of TEBA were smaller than those used in its absence, reflecting the inhibiting effect exerted by the additive. Furthermore, the fact that the activation coefficients ($b_1$ and $b_2$ from Table 3) of the charge transfer reactions are identical in the absence and in the presence of TEBA corroborates the relative invariance of the $IR_{ct}$ product (Figure 5B) again confirming the inhibiting effect of the investigated additive.

The differences between the simulated and experimental data, observed in the case of impedance spectra as well as of steady-state hydrodynamic voltammograms, may be due to the continuous increase in the active surface area during copper electrodeposition as well as to the neglect of the nucleation-growth contribution in the overall process.

## 5. Conclusions

The influence of TEBA on the kinetics of copper electrodeposition was interpreted in terms of a reaction model, based on the following:

(i) Two-electrochemical steps identical to those accepted in the absence of the additive.
(ii) The TEBA behaviour as a blocking agent, competing with cuprous ions for the active sites of the cathodic surface.
(iii) Neglecting the copper nucleation growth process. The experimental results obtained from hydrodynamic voltammetry at a rotating disc electrode and electrochemical impedance measurements were found to be in good agreement with those calculated on the basis of this reaction model.

## Acknowledgements

We are grateful to Dr R. Wiart and to Dr C. Cachet from UPR 15 du CNRS, Paris, for helpful discussions concerning the simulation. The contribution of Dr A. Nicoarã from 'Babes-Bolyai' University, Cluj-Napoca, to the interpretation of the experimental data is gratefully acknowledged. We thank CNCSIS (grant A 100/1074/2001) for financial support.

## References

1. D.F. Suarez and F.A. Olson, *J. Appl. Electrochem.* **22** (1992) 1002.
2. G. Fabricius, K. Kontturi and G. Sundholm, *Electrochim. Acta* **39** (1994) 2353.
3. M. Alodan and W. Smyrl, *Electrochim. Acta* **44** (1998) 299.
4. P. Cofré and A. Bustos, *J. Appl. Electrochem.* **24** (1994) 564.
5. Fabricius, K. Kontturi and G. Sundholm, *J. Appl. Electrochem.* **26** (1996) 1179.
6. B. Ke, J.J. Hoekstra, B.C. Jr Sison and D. Trivich, *J. Electrochem. Soc.* **109** (1962) 798.
7. Z.D. Stankovic, *Erzmetall* **38** (1985) 361.
8. Z.D. Stankovic and M. Vukovic, *Electrochim. Acta* **41** (1996) 2529.
9. D.R. Turner and G.R. Johnson, *J. Electrochem. Soc.* **109** (1962) 918.
10. D.R. Turner and G.R. Johnson, *J. Electrochem. Soc.* **109** (1962) 798.
11. E.E. Farnodon, F.C. Walsh and S.A. Campbell, *J. Appl. Electrochem.* **25** (1995) 574.
12. L. Muresan, S. Varvara, G. Maurin and S. Dorneanu, *Hydromet.* **54** (2000) 161.
13. S. Varvara, A. Nicoara, L. Mureşan, G. Maurin and I.C. Popescu, *Mater. Chem. Phys.* **72** (2001) 332–336.
14. M.A. Alodan and W.H. Smyrl, *J. Electrochem. Soc.* **145** (1998) 957.
15. B.C. Tripathy, S.C. Das, G.T. Hefter and P. Singh, *J. Appl. Electrochem.* **28** (1998) 915.
16. S. Varvara, B. Gabel and L. Muresan, Analele Universităţii din *Oradea*, Fascicola Chimie **VII** (2000) 38.
17. C. Cachet, R. Wiart, I. Ivanov, Y. Stefanov and S. Rashkov, *J.Appl. Electrochem.* **24** (1994) 713.
18. E. Mattson and O.M. Bockris, *Trans. Faraday. Soc.* **55** (1960) 1586.
19. T.I. Quickenden and X. Jiang, *Electrochim. Acta* **29** (1984) 693.
20. S. Goldbach, W. Messing, T. Daenen and F. Lapicque, *Electrochim. Acta* **44** (1988) 323.
21. M. Degrez and R. Winand, *Electrochim. Acta* **29** (1984) 365.

22. L. Muresan, A. Nicoara, S. Varvara and G. Maurin, *J. Appl. Electrochem.* **29** (1999) 719.
23. E. Chassaing and R. Wiart, *Electrochim. Acta* **29** (1984) 649.
24. R. Wiart, *Electrochim. Acta* **35** (1990) 1587.
25. R. Ichino, C. Cachet and R. Wiart, *Electrochim. Acta* **41** (1996) 1031.
26. F. Ganne, C. Cachet, G. Maurin, E. Chauveau and J. Petitjean, *J. Appl. Electrochem.* **30** (2000) 665.
27. J.J. Kelly and A.C. West, *J. Electrochem. Soc.* **145** (1998) 3477.
28. D.K.Y. Wong, B.A.W. Coller and D.R. MacFarlane, *Electrochim. Acta* **38** (1993) 2121.